The determination of the elastic constants of isotropic solids by means of transient thermal surface gratings

J. Fivez[1]

KU Leuven, campus Brussels, Warmoesberg 26, B-1000 Brussels, Belgium

(Dated: 25 November 2015)

Starting from the coupled thermoelastic equations, an analytic formula is obtained for the surface deformation of a semi-infinite homogeneous and isotropic solid in an impulsive stimulated scattering (ISS) experiment. The surface ripple consists of a transient diffusive grating and a standing Rayleigh wave. The time evolution of the diffusive part directly reveals the thermal diffusivity. The oscillatory part then reveals the elastic properties, and explicit formulae are presented for retrieving the elastic moduli as a function of the frequency and amplitude of the standing Rayleigh wave. The analytic formulae not only allow to avoid time-consuming and delicate numerical integration, but they also demonstrate the uniqueness of the inversion from signal to material parameters and offer direct insight into the error propagation. The formulae are applied to real experimental data, illustrating the strength and the limitations of the ISS technique.

PACS numbers: 78.20.nb, 81.70.Cv, 78.47.jj, 62.20.D-, 66.30.Xj

Keywords: photoacoustic, impulsive stimulated scattering, thermal grating, thermoelastic, elastic constants

I. INTRODUCTION

From a technical point of view, the elastic and thermal parameters of a material are very important, and several methods for the determination of these parameters have seen the light. One of these methods is impulsive stimulated scattering (ISS).[1–5] It relies on the creation of a transient grating at the surface of a specimen through the absorption of a laser light impulse and the resulting thermal expansion. The grating can then be probed in several ways, e.g. by measuring the efficiency of first order light diffraction, preferably in a heterodyne diffraction setup.[6] This article will not further address the problem of probing the grating, which has been discussed thoroughly before.[7] Rather, the focus will be on the grating profile itself and its relation to the material parameters.

Due to the impulsive creation of the thermal grating, the surface ripple representing the grating oscillates rapidly around its average profile. In this way, the transient thermal grating can seen as the superposition of two parts. The first part is a diffusive part, corresponding to the average profile and relatively slowly decaying due to thermal diffusion. The evolution of this part therefore is governed by the thermal diffusivity of the material. The second part is a standing surface wave. The amplitude and frequency of this part depend on the elastic properties. The analysis of the material then amounts to an inverse problem, i.e. retrieving thermal diffusivity and elastic constants from the ripple behavior.

The calculation of the magnitude of the excited ripple as a function of the material parameters is based on the solution of a set of coupled thermoelastic equations subject to the appropriate boundary conditions. For the general case, these equations are very complicated and have to be solved numerically. However, some attempts have been made to obtain analytical results. Käding et al.[8] considered the low-frequency limit of the coupled thermoelastic equations to calculate the diffusive part of the grating. For a homogeneous, isotropic semi-infinite material, they found that the time-dependence of the normal displacement was described by a complementary error function, with a characteristic decay time depending only on the applied grating spacing and the thermal diffusivity of the material. Until now, however, no simple explicit analytical formulae seem to have been derived for the oscillatory part of the grating.

In this paper, it is shown that the full ripple profile can be calculated analytically for homogeneous, isotropic semi-infinite materials. Such a result is important for several reasons.

First of all, analytical results are interesting in their own right, because they allow a general insight into the relation between material parameters and the ripple. They allow general conclusions about the uniqueness and error propagation of a solution to the inverse problem. And they offer a reference for the evaluation of numerical techniques, which remain necessary for inhomogeneous or layered materials.

This paper is organized as follows. In Sec. II explicit analytical formulae are developed for the diffusive and oscillatory part of the surface ripple as a function of the material parameters. In Sec. III explicit inverse formulae for the elastic constants as a function of the ripple frequency and amplitude are presented, and the error propagation is discussed. Then the method is successfully applied to experimental data. Sec. IV summarizes the conclusions.

II. THE FORWARD PROBLEM

A. The thermoelastic equations

Consider a semi-infinite homogeneous and isotropic bulk material, with a plane front surface at $y = 0$ absorbing a heat pulse of spatially periodic intensity

$$I(x,t) = q_{\mathrm{pu}}\delta(t)[1+\cos(Kx)], \tag{1}$$

where K is the wavenumber of the intensity variation along the x-axis. In reaction to the incident pump energy, surface displacements are initiated through the interaction of thermal and elastic properties. If the heating produced by the mechanical deformations is negligible, these are governed by the following set of coupled thermo-elastic differential equations for the temperature $T(x,y,t)$ and the displacement $\mathbf{u}(x,y,t)$ of the material[9]

$$\frac{1}{\alpha}\frac{\partial T}{\partial t} - \nabla^2 T = 0 \ , \tag{2}$$

$$\ddot{\mathbf{u}} - c_T^2\nabla^2\mathbf{u} - \left(c_L^2 - c_T^2\right)\nabla\left(\nabla\cdot\mathbf{u}\right) = -\gamma\nabla T \ , \tag{3}$$

where α is the thermal diffusivity, c_L and c_T are the longitudinal and transverse bulk wave velocities, and the thermo-elastic coupling constant is given by $\gamma = (3c_L^2 - 4c_T^2)\,\alpha_{\mathrm{th}}$, where α_{th} is the linear thermal expansion coefficient. Equations 2–3 must be solved subject to the boundary conditions at the free surface, specifying the heat flux at the surface $y = 0$ with

the y-axis pointing outward

$$\kappa \frac{\partial T}{\partial y}\bigg|_{y=0} = I(x,t) \ , \tag{4}$$

where κ is the thermal conductivity, and zero stress[10]

$$\sigma_{xy}|_{y=0} = \rho c_T^2 \left(\frac{\partial u_x}{\partial y} + \frac{\partial u_y}{\partial x} \right)\bigg|_{y=0} = 0 \ , \tag{5}$$

$$\sigma_{yy}|_{y=0} = \rho \left(\left(c_L^2 - 2c_T^2 \right) \frac{\partial u_x}{\partial x} + c_L^2 \frac{\partial u_y}{\partial y} \ - \gamma T \right)\bigg|_{y=0} = 0 \ , \tag{6}$$

where ρ is the mass density of the material. The ripple height is then equal to the displacement $u_y(x, y = 0, t)$. In principle, the in-plane displacement u_x could thereby distort the ripple form. However, since in practice the displacements are much smaller than the wavelength of the ripple, this is a negligible second order effect.

Using the Helmholtz decomposition of the displacement $\vec{u}$ in terms of a scalar longitudinal and a vectorial transverse displacement potential φ and $\vec{\psi} = (0, 0, \psi)$, Verstraeten et al.[7] derived a full formal solution for $u_y(x, y = 0, t)$. For absorption restricted to the surface $y = 0$ (i.e. optical absorption coefficient $\beta = \infty$), this solution reads as

$$u_y(x, y = 0, t) = A(t) \cos(Kx) \ , \tag{7}$$

where the time-modulated amplitude $A(t)$ is given by

$$A(t) = \int_{-\infty}^{+\infty} e^{i\omega t} \left(p_L(\omega)\varphi_1(\omega) + \sigma(\omega)\varphi_2(\omega) - iK\psi_1(\omega) \right) d\omega \ , \tag{8}$$

with

$$p_{L,T}(\omega) = \sqrt{K^2 - \omega^2/c_{L,T}^2} \ , \tag{9}$$

$$\sigma(\omega) = \sqrt{K^2 + i\omega/\alpha} \ , \tag{10}$$

$$\varphi_2(\omega) = \frac{\gamma q_{\mathrm{pu}}}{2\pi c_L^2 \kappa \sigma \left(\sigma^2 - p_L^2 \right)} \ , \tag{11}$$

$$\begin{pmatrix} \varphi_1 \\ \psi_1 \end{pmatrix} = -\frac{\varphi_2}{D_R} \begin{pmatrix} K^2 + p_T^2 & 2iKp_T \\ -2iKp_L & K^2 + p_T^2 \end{pmatrix} \cdot \begin{pmatrix} K^2 + p_T^2 \\ 2iK\sigma \end{pmatrix} \ , \tag{12}$$

$$D_R(\omega) = (K^2 + p_T^2)^2 - 4K^2 p_T p_L \ . \tag{13}$$

Equation 8 can then be simplified to

$$A(t) = \frac{\gamma q_{\mathrm{pu}}}{2\pi\kappa c_{\mathrm{T}}^4} \int_{-\infty}^{\infty} \frac{\omega \left(\omega^2 - 2K^2 c_{\mathrm{T}}^2 \right) \left(1 - p_{\mathrm{L}}(\omega)/\sigma(\omega) \right)}{\left(\omega + ic_{\mathrm{L}}^2/\alpha \right) D_R(\omega)} e^{i\omega t} \, d\omega \, . \tag{14}$$

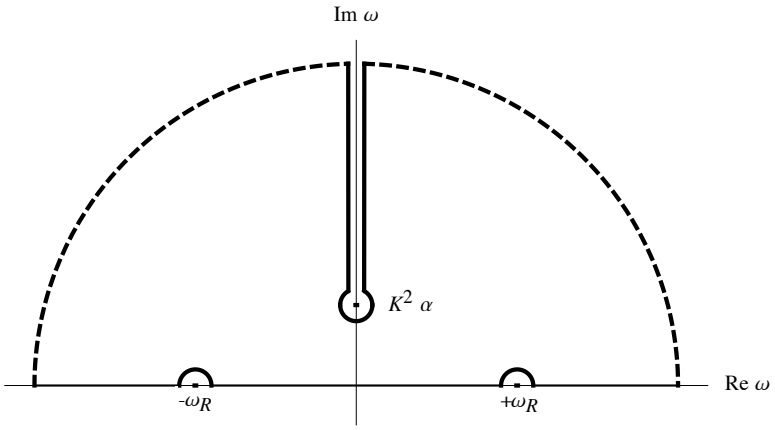

FIG. 1. The contour used for the evaluation of the ripple amplitude.

The integral in Eq. 14 can be evaluated by contour integration[11] using the infinite contour shown in Fig. 1, which circumvents the singularities of the integrand. The first singularity is the branch point $\sigma = 0$, located at $\omega = iK^2\alpha$, and the integral along the branch cut starting from the branch point then yields the damped diffusive part $A_d(t)$ of the ripple. The other two singularities are the non-trivial zeros $\pm\omega_R$ of the Rayleigh determinant D_R. Here, the Rayleigh angular frequency ω_R is the angular frequency of the arising standing surface wave, and is related to the non-dispersive Rayleigh wave velocity $c_R = \omega_R/K$. The integral over the semicircles around $\pm\omega_R$ then yields the oscillatory term $A_o(t)$ of the ripple amplitude. In the following, the diffusive and oscillatory terms will be treated separately.

B. The diffusive part of the thermal grating

With the coordinate transformation $\omega = iK^2\alpha u$ along the branch cut, the damped part $A_d(t)$ of Eq. 14 can be written as

$$A_d(t) = \frac{\gamma q_{\mathrm{pu}}}{\pi\kappa}\tau \int_1^\infty \frac{\sqrt{1+u^2\Gamma R/\delta^2}\; u\left(u^2+2\delta^2/R\right)/\left(u+\delta^2/(\Gamma R)\right)}{\left(u^2+2\delta^2/R\right)^2 - 4(\delta^2/R)\sqrt{u^2+\delta^2/R}\sqrt{\Gamma u^2+\delta^2/R}} \frac{e^{-ut/\tau}}{\sqrt{u-1}}\, du\,, \quad (15)$$

with

$$\tau = 1/(K^2\alpha)\ , \quad (16)$$

$$\delta = \omega_R\tau = c_R/(K\alpha), \quad (17)$$

$$R = c_R^2/c_T^2\ , \quad (18)$$

$$\Gamma = c_T^2/c_L^2\ . \quad (19)$$

Remark that R and Γ are not mutually independent, but are related by the Rayleigh condition $D_R(\omega_R) = 0$, which can be rewritten as

$$(2 - R)^2 = 4\sqrt{1 - R}\sqrt{1 - \Gamma R} \,, \tag{20}$$

yielding

$$\Gamma = \frac{R^3 - 8R^2 + 24R - 16}{16(R - 1)} \,. \tag{21}$$

Now, from elasticity it can be shown that Γ can be expressed in terms of the Poisson ratio ν of the material by[12]

$$\Gamma = \frac{1 - 2\nu}{2 - 2\nu} \,. \tag{22}$$

For all materials, the Poisson ratio satisfies the inequality $-1 < \nu < 0.5$, which implies that $0 < \Gamma < 0.75$ and $0.475 < R < 0.913$. Moreover, for most materials $0 < \nu < 0.5$ and hence $0 < \Gamma < 0.5$ and $0.764 < R < 0.913$.

For arbitrary values of δ, the integral in Eq. 15 cannot be calculated analytically. But for common grating wavelengths in an ISS experiment, the Rayleigh oscillations are very fast compared with thermal relaxation, and therefore δ is a very large number. Then Eq. 15 can be approximated by its limit for large δ, which can be written as

$$A_{d,\infty}(t) = C_d \,\mathrm{Erfc}(\sqrt{t/\tau}) \,, \tag{23}$$

where the initial magnitude C_d is given by

$$C_d = \frac{\gamma q_{\mathrm{pu}}}{\rho c(c_L^2 - c_T^2)} \,, \tag{24}$$

where c is the specific heat and $\mathrm{Erfc}(x)$ denotes the complementary error function.[13] Equation 23 coincides with the result of Käding et al.,[8] which was obtained by the exclusion of oscillations by omitting the time derivative in Eq. 3. It turns out that for $\delta > 100$ the approximation of $A_d(t)$ by $A_{d,\infty}(t)$ is very good, which justifies the use of $A_{d,\infty}$ as the diffusive term in the following. The time behavior of the diffusive part of the ripple then directly reveals the characteristic diffusion time τ. C_d depends on several material parameters and on the absorbed pump energy, and therefore does not allow the unambiguous retrieval of a single parameter.

C. The oscillatory part of the thermal grating

The oscillatory part of Eq. 14 can be written as

$$A_o(t) = \frac{\gamma q_{\mathrm{pu}}}{2\pi\kappa c_{\mathrm{T}}^4}(I_+(t) + I_-(t)) \ , \tag{25}$$

where $I_+(t)$ denotes the integral over the semicircle around $+\omega_R$, and I_- denotes the integral over the semicircle around $-\omega_R$. I_+ can now be calculated as follows

$$\begin{aligned} I_+(t) &= \lim_{\omega\to+\omega_R}\int_0^\pi \frac{\omega_R\left(\omega_R^2 - 2\omega_{\mathrm{T}}^2\right)\left(1 - p_{\mathrm{L}}(\omega_R)/\sigma(\omega_R)\right)}{\left(\omega_R + ic_{\mathrm{L}}^2/\alpha\right)D_R(\omega)} e^{i\omega_R t} i(\omega-\omega_R)d\theta \\ &= i\pi\frac{\omega_R\left(\omega_R^2 - 2\omega_{\mathrm{T}}^2\right)\left(1 - p_{\mathrm{L}}(\omega_R)/\sigma(\omega_R)\right)}{\left(\omega_R + ic_{\mathrm{L}}^2/\alpha\right)D'_R(\omega_R)} e^{i\omega_R t} \ , \end{aligned} \tag{26}$$

and I_- turns out to be the complex conjugate of I_+. Using Eqs. 13, 18–19 and 21, the derivative $D'_R(\omega_R)$ is found to be

$$D'_R(\omega_R) = \omega_R\left(\omega_R^2 - 2\omega_{\mathrm{T}}^2\right)\frac{R(2R^3 - 11R^2 + 16R - 8)}{(1-R)(2-R)^3 c_T^4} \ , \tag{27}$$

and the oscillatory part of the ripple amplitude then reads as

$$A_o(t) = \frac{\gamma q_{\mathrm{pu}}}{\kappa}\frac{(2-R)^3(1-R)\,\mathrm{Im}\left(\frac{1-\frac{p_L(\omega_R)}{\sigma(\omega_R)}}{\omega_R + ic_L^2/\alpha}\, e^{i\omega_R t}\right)}{R\left(-2R^3 + 11R^2 - 16R + 8\right)} \ . \tag{28}$$

Combination of Eqs. 28, 9–10, 16–19 and 21 then yields

$$A_o(t) = \frac{\gamma q_{\mathrm{pu}}}{\kappa}\frac{(R-2)^3\left(R^3 - 8R^2 + 24R - 16\right)\mathrm{Im}\left(\frac{1-(R/2-1)^2/(\sqrt{1+i\delta}\sqrt{1-R})}{\Gamma R + i\delta} e^{i\omega_R t}\right)}{16\left(2R^3 - 11R^2 + 16R - 8\right)\omega_R} \ . \tag{29}$$

Just as the diffusive part $A_d(t)$, the oscillatory part $A_o(t)$ of the ripple can commonly be approximated by its limit for large δ, which can be written as

$$A_{o,\infty}(t) = C_o\,\cos\left(Kc_R t\right) \ , \tag{30}$$

where

$$C_o = \frac{\gamma q_{\mathrm{pu}}}{\rho c\, c_R^2}\frac{(2-R)^3\left(R^3 - 8R^2 + 24R - 16\right)}{16\left(2R^3 - 11R^2 + 16R - 8\right)} \ . \tag{31}$$

It is clear that the observation of the time dependence directly reveals the Rayleigh velocity. C_o depends on several material parameters and on the absorbed pump energy, and therefore does not allow the unambiguous retrieval of a single parameter.

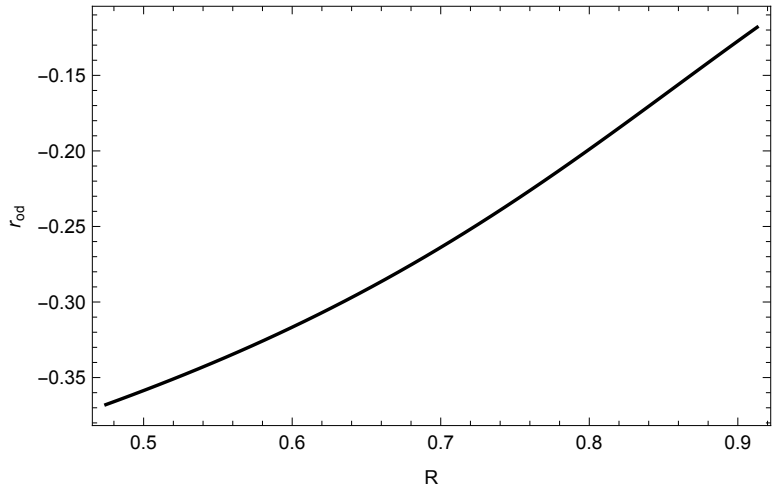

FIG. 2. The ripple ratio r_{od} as a function of R.

III. THE INVERSE PROBLEM

A. From ripple to material parmeters

As already discussed, comparison of Eqs. 23 and 30 with the time dependence of the experimental response in an ISS experiment gives direct access to the thermal diffusivity and the Rayleigh velocity. As homogeneous isotropic materials have two independent elastic parameters, for the full elastic characterization one supplementary parameter has to be determined in addition to c_R. This parameter can be retrieved from the ripple ratio $r_{od} = C_o/C_d$, which according to Eqs. 24 and 31 is given by

$$r_{od} = \frac{(2-R)^3\,(R^2-8R+8)}{16\,(2R^3-11R^2+16R-8)}\ , \tag{32}$$

which only depends on R, and is restricted to $-0.3679 < r_{od} < -0.1184$. For materials with positive Poisson ratio, r_{od} is even further limited to $-0.2236 < r_{od} < -0.1184$, meaning that in general the amplitude of the oscillatory part of the ripple will lie between 12 and 22% of the diffusive background. The fact that r_{od} is always negative can be understood by realizing that the ripple baseline is driven by thermal expansion, whereas the superposed Rayleigh wave is driven by inertia. As the thermal expansion pushes material away impulsively, inertia tries to counter this, resulting in material compression starting off the Rayleigh oscillation in antiphase.

Fig. 2 shows that the dependence of r_{od} on R is monotonous, which means that it can be inverted, allowing the easy retrieval of R from r_{od}. R then allows to determine the elastic

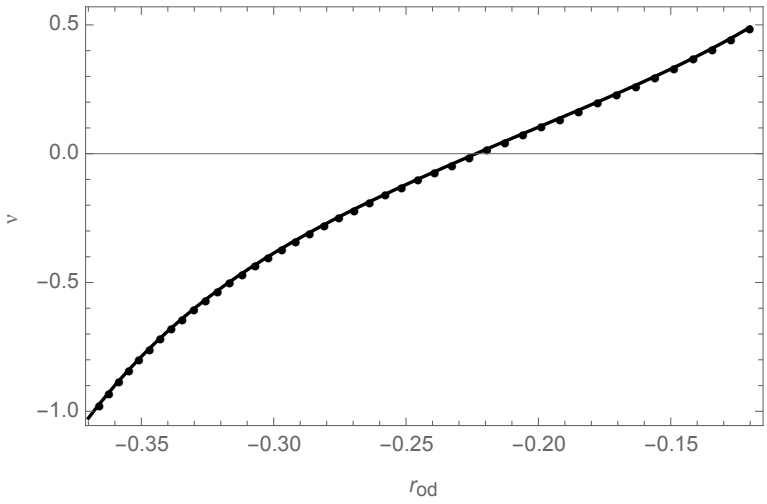

FIG. 3. Some couples (ν, r_{od}) together with their approximate polynomial relation.

constants as follows. From Eqs. 21–22 the Poisson ratio ν is found to be

$$\nu = \frac{R^3 - 8R^2 + 16R - 8}{R\,(R^2 - 8R + 8)} \ . \tag{33}$$

The Young modulus E is then given by[12]

$$E = 2\rho\, c_T^2(1+\nu) = \rho\, c_R^2\ \frac{4\,(R^3 - 8R^2 + 12R - 4)}{R^2\,(R^2 - 8R + 8)} \ . \tag{34}$$

This shows that the Young modulus can be determined from the ripple, as the density of a homogeneous sample can easily be measured.

A possible procedure for the retrieval of the elastic constants is then to determine r_{od}, numerically inverting it to R, and then applying Eqs. 33–34. However, since R has only a limited range, it is easy to combine Eqs. 33–34 with Eq. 32 into approximate polynomial expressions for ν and E as a function of r_{od}. In this way, the relation between the Poisson ratio and the ripple ratio is very well described by the polynomial

$$\nu = 2.23342 + 30.2654\, r_{od} + 214.193\, r_{od}^2 + 901.482\, r_{od}^3 + 1967.52\, r_{od}^4 + 1816.51\, r_{od}^5 \ , \tag{35}$$

with an inaccuracy generally much less than 5 per mil, which is negligible compared with experimental measuring errors. Figure 3 shows a number of couples (ν, r_{od}) together with the polynomial approximation. Remark that the relation is nearly linear in the most important region $\nu > 0$. The Young modulus can be adequately calculated from c_R and r_{od} using the

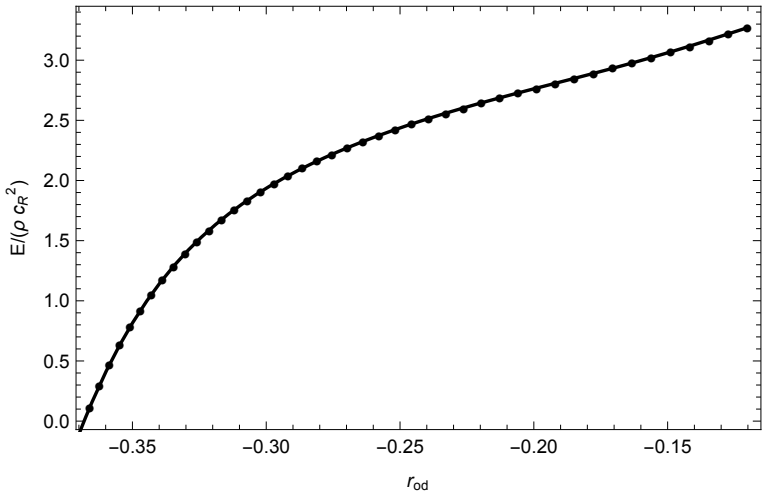

FIG. 4. Some couples $(E/(\rho\, c_R^2), r_{od})$ together with their approximate polynomial relation.

polynomial

$$E/(\rho\, c_R^2) = -128.652\, r_{od} - 1792.53\, r_{od}^2 - 12129.6\, r_{od}^3 - 44512.4\, r_{od}^4 - 85025.8\, r_{od}^5 - 67069.8\, r_{od}^6 \ , \tag{36}$$

again with an inaccuracy generally much lower than 5 per mil. Figure 4 shows a number of couples $(E/(\rho\, c_R^2), r_{od})$ together with the polynomial approximation. Again the relation is almost linear in the most important region. The retrieval of the elastic constants from the surface ripple is now as easy as determining the ratio r_{od} and c_R, and then applying Eqs. 35–36.

B. Error analysis

Equations 35–36 not only facilitate the straightforward retrieval of the elastic constants from the ISS signal, they also provide direct insight into the expected experimental error. Here we restrict the discussion to materials with positive Poisson ratio.

As seen, the relation between ν and r_{od} is then more or less linear, with an average derivative around 5, and hence the uncertainty $\Delta\nu$ can be written as

$$\Delta\nu \approx 5\Delta r_{od} \ . \tag{37}$$

Since a realistic experimental uncertainty in r_{od} probably will not be better than $\Delta r_{od} \approx 0.01$, one can expect the uncertainty in the Poisson ratio to be $\Delta\nu \approx 0.05$ at best.

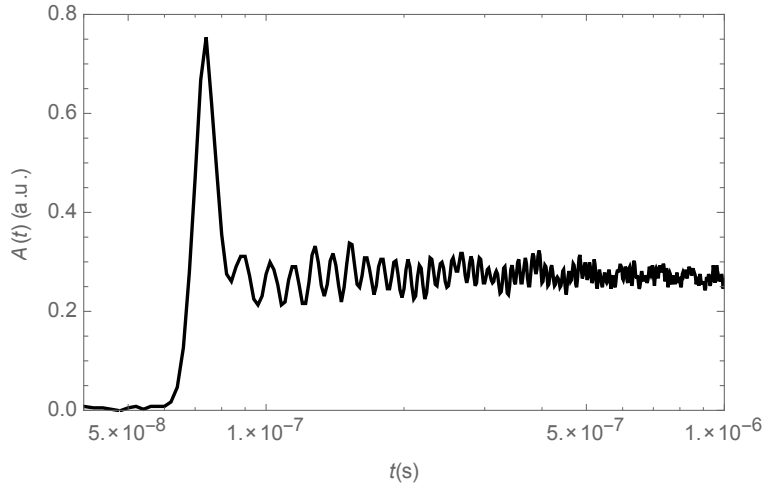

FIG. 5. Time dependence of the ripple magnitude of a 40 μm thermal grating on the surface of a glass substrate covered with a thin aluminum layer.

In the region of positive ν, the relation between $E/(\rho\, c_R^2)$ and r_{od} is also more or less linear, with a derivative around 6.5, and hence the uncertainty on $E/(\rho\, c_R^2)$ approximately reads as

$$\Delta\left(\frac{E}{\rho\, c_R^2}\right) \approx 6.5 \Delta r_{od} \ , \tag{38}$$

yielding a relative uncertainty of about 3% in E if $\Delta r_{od} \approx 0.01$.

C. Experimental validation

In order to validate the procedure for the retrieval of the elastic parameters, it was applied to a set of real experimental measurements. In this experiment,[7] a 40 μm thermal grating was created on the surface of a mirror plate of an unknown glass, coated with an aluminum layer with a thickness of 100 nm increasing the optical reflection and restricting the heat absorption to the very surface. As the coating thickness is much less than the grating period, its influence on the ISS outcome is negligible. The experimental data consist of a set of 6 measurements, and Fig. 5 shows one of the signals during the first microsecond. The first part is sufficient, since we focus on the retrieval of the elastic parameters and therefore do not need the tail dominated by thermal diffusion. The short initial peak is no real part of the ISS signal. A comparable peak has been found by other authors and attributed to electronic excitation and decay.[14] Besides the Rayleigh oscillations, slow interfacial Scholte

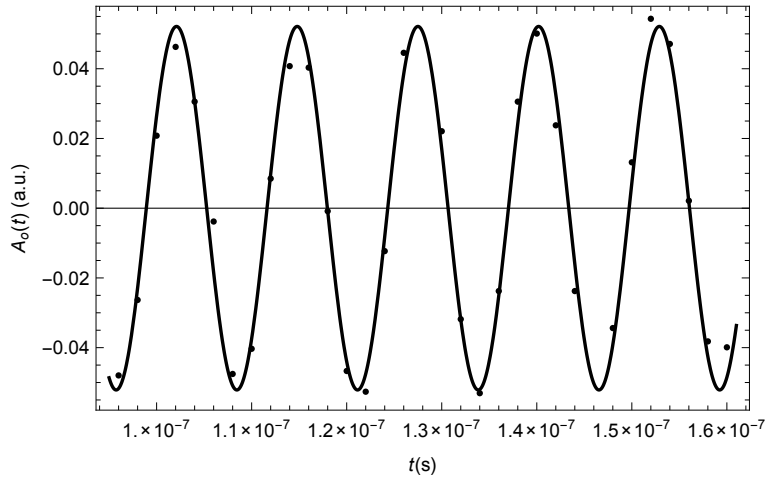

FIG. 6. The Rayleigh oscillations contained in the signal of Fig. 5, together with their best fit.

oscillations are present,[15] which are known to travel at the speed of sound in air and hence offer a way to verify the grating wavelength. On the other hand, because of their much lower amplitude and frequency, their energy content is negligible and therefore they do not influence the outcome of the analysis.

The data was analyzed as follows. For each signal, the Rayleigh oscillation was obtained by subtracting the background, which was calculated as the moving average over one Rayleigh period. For the sake of accuracy, the Rayleigh velocity c_R was determined by measuring the first ten stable oscillations after the initial peak. For the determination of the ratio r_{od}, only the first five oscillations were used in order to avoid influence from damping, and their amplitude was divided by the background. Fig. 6 shows the best fitting cosine for the data set of Fig. 5, giving an impression of the fit quality. The Rayleigh velocity and ripple ratio were extracted for the six signals and then averaged, yielding $c_R = (3150 \pm 40)\mathrm{m/s}$ and $r_{od} = -0.177 \pm 0.012$. It then follows that $\delta > 10^4$, which justifies the use of the limit for infinite δ.

The next step was to use Eqs. 35–36 to calculate the elastic constants. Table I compares the calculated values of the elastic constants with reference values for some glass types. The sample parameters nicely match those of a crown glass. We conclude that the ISS signal allowed to adequately probe the glass through the thin aluminum layer.

TABLE I. Retrieved elastic constants for the glass sample together with reference values for some different glass types.

glass type	$\boldsymbol{\rho}$ (kg/m^3)	$\boldsymbol{E}$ (GPa)	$\boldsymbol{\nu}$ (–)
crown glass[a]	2550	71.5	0.21
fused silica[a]	2200	73	0.16
soda lime[a]	2440	72	0.22
boroslicate[a]	2230	64	0.20
sample	2510±20	72±2	0.21±0.06

[a] `www.cidraprecisionservices.com/products-services-materials-we-machine-glass.html`.

IV. CONCLUSIONS

Already in 1995 Käding et al. demonstrated the practical use of ISS for the determination of the thermal diffusivity of bulk material with a flat surface by fitting a complementary error function to the observed thermal decay of the excited thermal grating. In this article, an equally simple direct way of extracting the elastic parameters from the ISS signal was presented.

The procedure amounts to the determination of the velocity c_R of the excited Rayleigh wave together with the ratio r_{od} of their amplitude to the non-oscillatory diffusive part of the excited grating. The theory shows that r_{od} completely determines the Poisson ratio of the material, which can be calculated conveniently and accurately by means of a polynomial. The Young modulus turns out to be the product of density, c_R^2 and a function of r_{od} that again can be calculated accurately by a polynomial. The dependence on the ripple ratio r_{od} rather than on absolute ripple heights makes the experimental aspect substantially easier.

Simple error analysis showed that even with good experimental data the expected experimental absolute uncertainty in the Poisson ratio is about 0.05, and the expected relative uncertainty for the Young modulus about 3%.

The application of the procedure to a set of ISS measurements on a glass sample proved its practical value, producing results in very good agreement with reference glass parameters, with an uncertainty in line with the expectations. It is interesting to notice that the actual measurement was done on a sample covered with a very thin aluminum coating. This

underlines the ability of the ISS technique to directly probe the elastic constants of a material concealed by a layer much thinner than the grating wavelength. This is because both thermal and Rayleigh waves have a penetration depth of the order of their wavelength. Although the ripple height is only of the order of picometer, it arises due to the expansion and oscillation of a much thicker region, with an effective thickness of about the thermal grating wavelength, which is of the order of tens of microns in the example. The coating is only a negligible part of this. Another consequence is that the assumption of semi-infiniteness is valid as soon as the specimen is much thicker than the thermal wavelength, which is true for the glass plate used for the experimental validation.

In conclusion, the proposed procedure provides an easy way to extract elastic parameters from an ISS experiment. Moreover, as it is based on exact formulae, it sets a benchmark for numerical methods, which of course still remain necessary for more complicated cases, such as for layered materials.

ACKNOWLEDGMENTS

The author is grateful to C. Glorieux for providing the experimental ISS data used for the validation.

REFERENCES

[1]H. Eichler, J. Mod. Optic. **24**, 631 (1977).

[2]Y. Yan, E. Gamble Jr, and K. Nelson, J. Chem. Phys. **83**, 5391 (1985).

[3]Y.-X. Yan and K. A. Nelson, J. Chem. Phys. **87**, 6240 (1987).

[4]K. A. Nelson, R. Miller, D. Lutz, and M. Fayer, J. Appl. Phys. **53**, 1144 (1982).

[5]J. Monchalin, IEEE T. Ultrason. Ferr. **33**, 485 (1986).

[6]A. Maznev, K. Nelson, and J. Rogers, Opt. Lett. **23**, 1319 (1998).

[7]B. Verstraeten, J. Sermeus, R. Salenbien, J. Fivez, G. Shkerdin, and C. Glorieux, Photoacoustics **3**, 64 (2015).

[8]O. Käding, H. Skurk, A. Maznev, and E. Matthias, Appl. Phys. A: Materials Science & Processing **61**, 253 (1995).

[9]A. Rosencwaig and A. Gersho, J. Appl. Phys. **47**, 64 (1976).

[10]A. Duggal, J. Rogers, and K. Nelson, J. Appl. Phys. **72**, 2823 (1992).

[11]H. W. Wyld, *Mathematical Methods for Physics*, edited by D. Pines, Lecture notes and supplements in physics, Vol. 15 (W. A. Benjamin, Reading, 1976).

[12]J. Achenbach, *Wave propagation in elastic solids* (North-Holland, Amsterdam, 1984).

[13]M. Abramowitz and I. A. Stegun, *Handbook of Mathematical Functions*, 9th ed. (Dover Publications, New York, 1972).

[14]E. V. Ivakin, M. U. Karelin, and A. V. Sukhadolau, J. Appl. Phys. **105**, 113107 (2009).

[15]V. Gusev, C. Desmet, W. Lauriks, C. Glorieux, and J. Thoen, J. Acoust. Soc. Am. **100**, 1514 (1996).